Dimerization of Tissue Factor Supports Solution-Phase Autoactivation of Factor VII without Influencing Proteolytic Activation of Factor X

F. Doñate,† C. R. Kelly,‡ W. Ruf, and T. S. Edgington*

Departments of Immunology and Vascular Biology, The Scripps Research Institute, La Jolla, California 92037

Received April 28, 2000; Revised Manuscript Received July 6, 2000

ABSTRACT: Tissue factor (TF) is a transmembrane receptor that initiates the thrombogenic cascade by assembly with the serine protease factor VII or VIIa (VII/VIIa) resulting in formation of the bimolecular active complex TF·VIIa. Chemical cross-linking studies identified that a minor population of TF forms dimers on the surface of cells, possibly influencing TF·VIIa proteolytic function as a result of dimerization. We here investigate the effects of dimerization of the extracellular domain of TF on the proteolytic function of the TF·VIIa complex. The leucine zipper dimerization domain of the yeast transcriptional factor GCN4 (LZ) was genetically fused at the C-terminus of the extracellular domain of TF separated by a short linker (TF_LLZ). TF_LLZ homodimerized with a K_d similar to that of the LZ peptide. Tryptophan fluorescence indicated that the two TF moieties were in close proximity and parallel orientation in TF_LLZ. TF_LLZ dimers bound two molecules of VIIa, and VIIa binding did not influence the TF dimer equilibrium. Dimerization influenced neither amidolytic nor the factor X activation activities of the TF·VIIa complexes. Notably, dimer TF_LLZ efficiently promoted the autoactivation of VII to VIIa in solution in contrast to monomeric TF_LLZ or TF_{1-218}. Thus, TF dimerization on cells may serve to "prime" the initiation of the coagulation pathway by generating active TF·VIIa complexes for the subsequent activation of downstream macromolecular substrates.

Tissue factor (TF[1]) is a cell surface transmembrane-anchored glycoprotein of 263 amino acids that initiates blood coagulation by acting as the cellular receptor and essential cofactor for the serine protease zymogen factor VII and its activated form, factor VIIa (VII/VIIa) (*1*−*3*). TF is structurally organized in three domains: an extracellular domain (residues 1−219), a transmembrane domain (residues 220−242), and a cytoplasmic domain (residues 243−263). The extracellular domain is constituted by the tandem association of two fibronectin type III-like modules (residues 4−209) and a flexible peptidyl strand (residues 210−220) that tethers the domain to the transmembrane anchor (*4*−*6*). The extracellular domain of TF binds both the latent protease VIIa and the zymogen precursor VII. One of the cofactor roles of TF is to enhance susceptibility to proteolytic activation of the bound zymogen VII by activating proteases, such as factor Xa and the TF·VIIa complex. In the latter case, the activation reaction is driven by the collision of TF·VIIa and TF·VII complexes by diffusion or directed association in phospholipid bilayers (*7*), suggesting the importance of proper parallel presentation of the TF-bound zymogen VII to the proteolytic VIIa in complex with another TF molecule. The more important recognized function of TF, when in binary complex with VIIa, is to allosterically induce function of the associated VIIa protease domain for full catalytic activity and to contribute to a remote macromolecular substrate docking exosite created by an extended region of both cofactor and enzyme (*1*−*3*). The TF·VIIa complex represents the major in vivo trigger of the coagulation pathways through limited proteolytic activation of the macromolecular substrate zymogens factor IX and X (*8*−*9*).

The activation of macromolecular substrates by TF·VIIa is highly dependent on localization of the complex in anionic phospholipid membranes to which the substrate Gla domain binds, thus facilitating mass transport and proper presentation of substrates to TF·VIIa. Similarly, TF·VIIa's proteolytic activity on the cell surface is subject to modulation by stimuli that influence the phospholipid asymmetry of the cell membrane, such as complement attack (*10*) or Ca^{2+} ionophore stimulation (*11*, *12*). However, the plasma membrane also contains specific, glycosphingolipid-rich microdomains in which the TF·VIIa complex has greatly diminished proteolytic activity. Since TF can traffic between areas of the membrane that are rich in anionic phospholipid or glycosphingolipid, regulation of function may result from the localization of the TF and TF·VIIa in different cell surface microdomains (*13*). A third mechanism was sug-

* Departments of Immunology and Vascular Biology, C204, 10550 N. Torrey Pines Rd., The Scripps Research Institute, La Jolla, CA 92037. Telephone: (858) 784-8225. Fax: (858) 784-8480. E-mail: tse@scripps.edu.

† Present address: NuVas LLC, 11545 Sorrento Valley Rd., Suite 305 B, San Diego, CA 92121.

‡ Present address: Alcon Laboratories, 6201 South Freeway, Forth Worth, TX 76134.

[1] Abbreviations: TF, tissue factor; VII, factor VII; VIIa, factor VIIa; VII/VIIa, coagulation factor VII/VIIa; TF·VII, binary complex of TF and VII; TF·VIIa, binary complex of TF and VIIa; X/Xa, coagulation factor X/Xa; IX, coagulation factor IX; LZ, leucine zipper of GCN4; LZP, leucine zipper peptide of GCN4; TBS, Tris-buffered saline; PBS, phosphate-buffered saline; CHAPS, 3-[93-cholamidopropyl)dimethylammonio]-1-propanesulfonate; BS^3, bis[sulfosuccinimidyl]suberate; DTSSP, 3,3′-dithiobis[sulfosuccinimidylpropionate].

10.1021/bi000986p CCC: $19.00
Published on Web 08/24/2000

gested from study of the hematopoietic HL60 cell line. As for other cell types (*14*), cell surface TF in these cells can chemically be cross-linked, indicating the existence of TF in very close approximation or in actual dimers on the cell surface. Enhancement of TF activity on HL60 cells by Ca ionophore stimulation was associated with diminished TF cross-linking, suggesting that dimer formation may influence TF·VIIa proteolytic function (*15*). Since the Lys residues in TF that are the primary target for amino-reactive cross-linkers (*16*, *17*) are located within the macromolecular substrate exosite, dimerization is inferred to cause steric hindrance at this essential exosite.

In this study, we have directly examined the effects of dimerization of the extracellular domain of TF on binding and cofactor functions by generating parallel oriented dimers of the TF extracellular domain in solution. To this end, we constructed hybrid molecules of TF that formed stable, but reversible dimers through the leucine zipper dimerization region of the yeast transcription activator GCN4 (LZ) which was fused at the C-terminus of the C module of the extracellular domain of TF (TF_{1-220}). Deduced from the known structure and the well-established function of the GCN4 dimerization domain (*18*), a parallel orientation will be imposed on the two extracellular domains of TF in the homodimeric molecule. Furthermore, the generation of a soluble dimeric molecule of TF permits direct biophysical analysis of the dimer−monomer transition by various techniques. The results demonstrate that dimerization of TF does not influence the proteolytic activity of the assembled TF·VIIa dimers toward the macromolecular substrate factor X. However, compared to monomeric soluble TF, zymogen VII activation was greatly enhanced in the presence of dimeric TF, suggesting that the parallel orientation of two TF molecules provides sufficient proximity of the TF bound VIIa enzyme and VII substrate for proper interaction even in the absence of a phospholipid surface.

EXPERIMENTAL PROCEDURES

TF_LLZ, TFLZ, and LZP Design, Refolding, and Purification. The cDNA of the leucine zipper domain of the yeast transcription factor GCN4 was obtained by PCR from yeast genomic DNA using the primer pair 5′atcggcggcgccgccatgaaacaacttgaagacaag and 5′gatcaaagctttcagcgttcgccaactaa. The 5′ primer incorporated a NarI site encoding for the linker sequence Gly−Gly−Ala−Ala followed by Met−Lys−Asn−Leu...., corresponding to the GCN4 dimerization domain starting at residue 2. The coding sequence for TF_{1-220} was amplified with primer 5′ggcggcgccgcctatttctcgaattcccc which introduces a NarI site at the 3′ end, resulting in an in-frame fusion protein from residue 220 of TF to the Gly−Gly−Ala−Ala linker that precedes GCN4, and primer 5′gaagaaggatcctggtgcctcgtggttctggcactacaaatact which includes a BamHI site for cloning in frame with the hexa−His sequence of pTrcHisC (Invitrogen) followed by a thrombin cleavage site (Val−Pro−Arg−Gly), as previously described (*19*). The two PCR fragments were digested with the respective endonucleases and ligated simultaneously into BamHI/HindIII-restricted pTrcHisC (*19*) resulting in the expression construct for TF_LLZ. To splice out the Gly−Gly−Ala−Ala linker sequence, the GCN4 and TF portions were separately amplified with oligonucleotides that created an overlap corresponding to the sequence Phe−Arg−Glu−Ala−Met−Lys−Asn−Leu, in which Glu corresponds to TF residue 219 and Met to GCN4 residue 2. In the process, Ile_{220} was mutated to Ala. By combining the two fragments in a PCR reaction with the outmost 5′ and 3′ primers, a full-length clone for the fusion protein TFLZ was obtained and subcloned into pTrcHisC. The GCN4 domain of TF_LLZ was amplified by PCR using a 3′ primer as described above and the 5′ primer 5′ataaggatccggtgcctcgtggcgccgccatgaaacaac for in-frame cloning into the BamHI site of pTrcHisB followed by sequences that encode for a thrombin cleavage site (Val−Pro−Arg−Gly) and an Ala−Ala spacer that precedes residue 2 of GCN4 to yield a construct for the GCN4 leucine zipper peptide LZP.

Recombinant protein was expressed in the *Escherichia coli* strain BL21, inclusion bodies were isolated and solubilized in guanidinium hydrochloride (GuHCl) (*19*). The protein was purified on a nickel-chelating column (Ni−NTA from Qiagen) on which the TF extracellular domain was folded by the use of a linear gradient from buffer A (6 M GuHCl, 0.5 M NaCl, and 20 mM sodium/potassium phosphate, pH 8.0) to buffer B (0.8 M GuHCl, 0.3 M NaCl, 50 mM Tris-HCl, 2.5 mM reduced glutathione, and 0.5 mM oxidized glutathione, pH 8.0) over a period of 8 h. The column was then washed extensively with 10 mM Tris and 20 mM NaCl, pH 7.5, and the protein eluted in the same buffer containing 250 mM imidazole. Where indicated, the His tag was removed by incubation with thrombin (10 μg/mg of protein) at 37 °C for 3 h. A final FPLC purification step on Mono Q yielded homogeneous protein based on SDS PAGE. To isolate the LZP after binding to nickel-chelating column, the column was extensively washed with 10 mM Tris and 20 mM NaCl, pH 7.5. The peptide was eluted with 250 mM imidazole in the same buffer. The thrombin digestion was performed as indicated above. A final reverse-phase chromatographic step in a Pharmacia 15 RPC HR 5/10 column was performed. The peptide was eluted using a water/acetonitrile (0−60%) gradient in 30 min. The final peptide preparation was lyophilized and stored at −80 °C. The purity and thrombin digestion of LZP were assessed after SDS−PAGE on 10−20% tricine gels, fixation with 10% TCA and Coomasie blue staining. Molecular weights for the proteins are as follows: TF_LLZ containing the His tag, 33 515; without tag, 29 050; TFLZ containing the His tag, 33 217; without tag, 28 752; and LZP containing the His tag, 8504; without tag, 4040. The protein concentration was determined by absorbance at 280 nm using extinction coefficients of 45 090 and 38 120 M^{-1} cm^{-1} for TF_LLZ and TFLZ with and without tag, respectively, and 8250 and 1280 M^{-1} cm^{-1} for the LZP with and without tag, respectively.

Chemical Cross-Linking and Western Blotting. Chemical cross-linking was performed with the bifunctional cross-linkers BS^3 and DTSSP (Pierce) at 2−4 mM for 30 min at room temperature in PBS (10 mM sodium phosphate, 150 mM NaCl, pH 7.5). The reaction was stopped by addition of Tris to 10 mM. The samples were separated on 8−16% gradient SDS−PAGE gels under nonreducing conditions unless indicated otherwise. The gels were silver-stained (Integrated Separation Systems), and staining intensities were quantified in a Molecular Dynamics gel scanner. Western blot analysis was performed as described (*13*). Briefly, the samples were transfer after SDS−PAGE onto Immobilon P (Millipore) using a semidry transblot system. TF was detected

with polyclonal goat anti-TF and VIIa with mAb F5−13B12. Bound primary antibodies were detected by appropriate HRP-conjugated secondary antibodies and visualized using chemiluminescence reagents from Amersham and exposure of X-Omat AR film (Eastman-Kodak).

Circular Dichroism (CD) Spectroscopy. CD was performed in a AVIS 61DS spectropolarimeter at room temperature with a cuvette size of 0.1 mm from 260 to 200 nm at 0.5 nm intervals and with a bandwidth of 1.5 nm. The spectra collected are the average of three recordings. The buffer consisted of 20 mM potassium phosphate and 10 mM NaCl, pH 7.4, and the protein concentration was 10 μM.

Fluorescence Spectroscopy. Fluorescence spectroscopy of the protein samples (2 μM) dissolved in TBS (10 mM Tris, 150 mM NaCl, pH 7.5) buffer was carried out in a SLM/Aminco AB2 spectrofluorometer. Four (Figure 4) or six (Figure 5) different spectra were recorded for each sample with a bandwidth at emission (em) and excitation (ex) of 4 nm. Samples were excited at $\lambda_{ex} = 296$ nm, and spectra were recorded from $\lambda_{em} = 300-400$ nm at 0.4 nm (Figure 4) or 0.6 nm (Figure 5) intervals.

Amidolytic Activity. The amidolytic activity of VIIa bound to TF was measured by incubating the indicated concentration of VIIa at 37 °C in TBS, 5 mM $CaCl_2$, and 0.02% BSA in a 96-well plate with TF_LLZ, TFLZ, or TF_{1-218}. Initial rates of hydrolysis of the chromogenic substrate Spectrozyme FXa (1.25 mM final concentration) were measured at 405 nm in a microplate reader (Molecular Devices).

Proteins. Purified human plasma-derived FVII was purchased from Haematologic Technologies. We produced recombinant FVIIa in Chinese hamster ovary cells. The protein was purified by sequential monoclonal antibody affinity and ion exchange chromatography and activated by autocatalytic conversion, as previously described (*20*, *21*). Human plasma-derived FX was purified and rendered free of FVII or FVIIa by affinity chromatography as previously described (*21*).

Proteolytic Activity. FXa generation was measured at 37 °C in TBS, 5 mM $CaCl_2$, and 0.02% BSA. VIIa was preincubated with increasing concentrations of TF_{1-218} or the respective dimeric TFs, followed by addition of FX to a final concentration of 1 μM. After the reaction was quenched with 100 mM EDTA, FXa generation was quantified with the chromogenic substrate Spectrozyme FXa (0.2 mM final concentration) at 405 nm in a microplate reader.

Autoactivation of VII. Autoactivation of VII was measured by incubating 300 nM of TF and, where indicated, a 50-fold molar excess of LZP with 300 nM VII in TBS buffer, 5 mM $CaCl_2$, and 0.02% BSA at 37 °C. Aliquots of 20 μL were taken immediately after the addition of VII and at the indicated times. The amidolytic activity of generated VIIa was assayed in a final volume of 200 μL as indicated above.

RESULTS

Engineered Soluble TF Dimers. Chemical cross-linking indicated that cell surface-expressed TF can dimerize (*14*), whereas the extracellular domain of TF has been shown to be monomeric in solution (*22*). To create a soluble dimeric TF protein, the leucine zipper dimerization domain of the yeast transcription factor GCN4 (LZ) was fused to the C-terminus of the extracellular domain of TF (amino acids 1−220), TF_LLZ (Figure 1) replacing the location of the transmembrane domain. This construct contains a short linker composed of Gly−Gly−Ala−Ala between the TF and LZ moieties to provide flexibility that avoids interference of TF with the dimerization function of the leucine zipper domain. In another hybrid molecule (TFLZ) (Figure 1), the linker was omitted to more closely mimic the dimerized state of TF in the cell membrane where the transmembrane domain was implicated as the mediator of the dimerized state (*14*). To quantitatively modulate the degree of dimerization of TF hybrid molecules, a peptide corresponding to the leucine zipper of GCN4 was expressed (LZP) (Figure 1). All of the proteins contain a His tag for purification purposes. The presence of additional residues at the N-terminus was demonstrated to be without effect on any of the analyzed properties, except the fluorescence measurements (Figure 3). Thus, experiments were carried out with the proteins containing the His tag unless otherwise indicated.

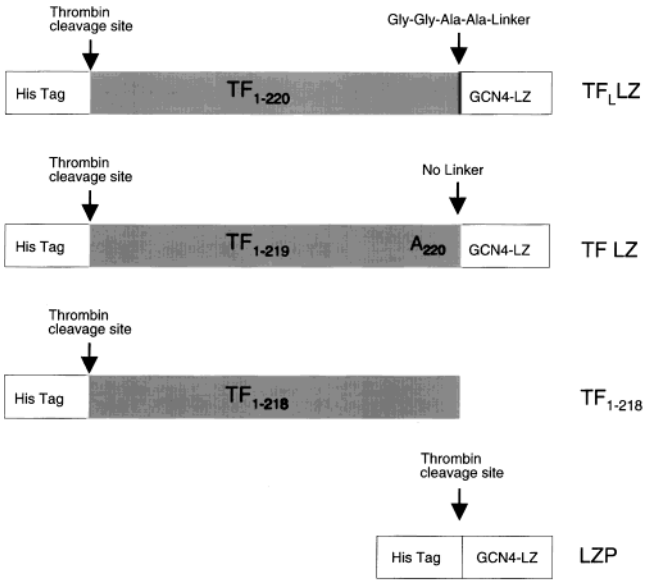

FIGURE 1: TF constructs. The hybrid construct TF_LLZ was cloned into the vector pTrc His C, containing a histidine tag for purification purposes at the N-terminus. A thrombin cleavage site was engineered between the His tag and TF_{1-220} which leaves an extra glycine residue after thrombin digestion. A short flexible linker (Gly−Gly−Ala−Ala) separated the C-terminus of TF_{1-220} from the leucine zipper of GCN4 (GCN4−LZ). This linker was removed in TFLZ and in the process, Ile_{220} was mutated to Ala. TF_{1-218} and GCN4−LZ (LZP) were also cloned into a vector containing a histidine tag and a thrombin cleavage site.

Determining the Dimeric Nature of TF_LLZ. The reversible dimerization of TF_LLZ, was verified by three independent methods: chemical cross-linking, measurement of α-helix formation of the leucine zipper domain by circular dichroism, and proximity-dependent effects on the intrinsic protein fluorescence.

TF_LLZ in solution was chemically cross-linked using the homobifunctional, aminoreactive cross-linkers DTSSP and BS^3, followed by SDS−PAGE and silver-stain display to determine the molecular weight of the cross-linked species (Figure 2). DTSSP contains a reducible internal disulfide bridge that permits dissociation of cross-linked molecules by chemical reduction. Figure 2A illustrates a typical cross-linking experiment with TF_LLZ, and by comparison in Figure 2B, a control cross-linking experiment with TF_{1-218} devoid

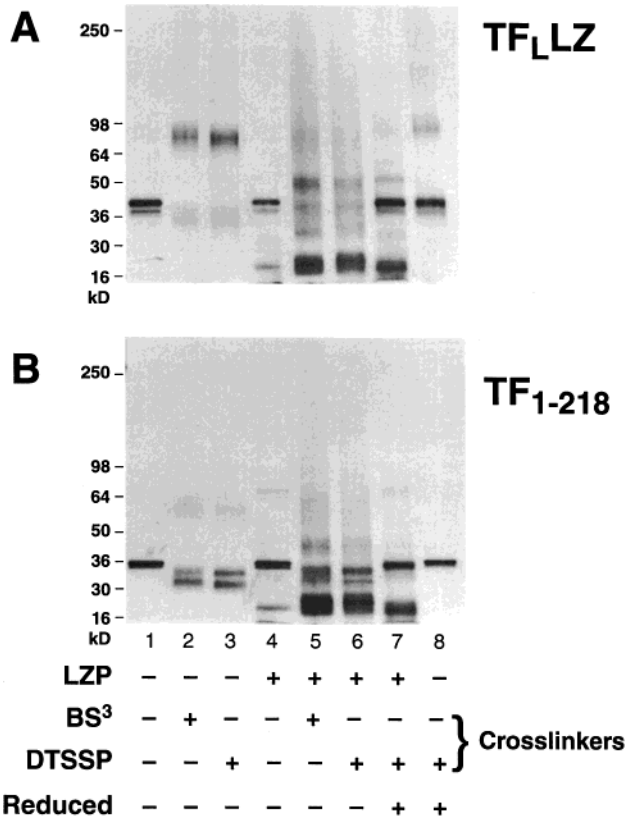

FIGURE 2: Chemical cross-linking of TF_LLZ shows that it is predominantly dimeric. Aliquots (4 μM) of TF_LLZ (A) or TF_{1-218} (B) were cross-linked for 30 min at room temperature with 2.5 mM of the bifunctional cross-linkers BS^3 (lanes 2 and 5) or DTSSP (lanes 3, 6, 7 and 8). Samples 4−7 were preincubated with a 10-fold molar excess of LZP. The reactions were stopped by adding Tris buffer. The cross-linking species were separated by 8−16% SDS PAGE under reducing (lanes 7 and 8) or nonreducing (lanes 1−6) conditions and detected by silver staining.

of a dimerization domain. Approximately 80% of TF_LLZ (Figure 2A) was cross-linked in a dimeric form of ~80 kD (compare lane 1 with lanes 2 and 3) with both cross-linkers, whereas TF_{1-218} remained monomeric (Figure 2B). Intramolecular cross-linking was evident from the faster electrophoretic mobility of the monomeric species following the cross-linking reaction. The amount of TF_LLZ dimer cross-linked was diminished in the presence of an excess of the LZP peptide (lanes 5 and 6). In the presence of LZP, the predominant species was a heterodimer of TF_LLZ with LZP (band of ~55 kD), whereas TF_{1-218} remained monomeric. The small amount of heterodimers of TF_{1-218} with LZP is interpreted as nonspecific cross-linking due to the high concentration of competing LZP. LZP also appears to undergo extensive cross-linking, as deduced from the broadening of the approximately 16 kD band (compare lanes 5 and 6 with lane 4), which represents residual SDS resistant dimers. Under reducing conditions, the intra- and intermolecular cross-linkings by the disulfide containing DTSSP were largely reversible (lanes 7 and 8). Thus, TF_LLZ is a dimer at the concentrations tested, and the equilibrium can be shifted to the monomeric form by addition of an excess of LZP.

LZP is α-helical in its dimeric form but unstructured as a monomer (*23*). Since the α-helical content of TF_{1-218} is negligible as derived from CD analysis (*19*, *24*), the dimer formation by TF_LLZ can be observed from the α-helical signal generated by the dimeric LZ domain. The CD spectrum (Figure 3A) of TF_LLZ exhibited two minima at ~208 and 222 nm, characteristic of high α-helical content, confirming the dimeric nature of TF_LLZ at that concentration. When the spectrum of the LZP was subtracted from that of TF_LLZ, the resulting spectrum was identical to that of TF_{1-218}, including the shoulder at 331 nm that was masked in the spectrum of TF_LLZ (Figure 3B). Therefore, the presence of the LZ domain at the C-terminus of TF_LLZ does not appear to induce structural changes in the TF extracellular domain as detected by CD.

The following experiment was performed with TF_{1-218} and TF_LLZ lacking the amino terminal His tag. The emission fluorescence spectra of tryptophans at $\lambda_{ex} = 296$ nm are shown in Figure 4A for TF_{1-218} and TF_LLZ. The LZ lacks Trp and consequently, the signal recorded for TF_LLZ was the result of two fluorescent tryptophans (residues 14 and 45) of the four present in the TF domain (*25*). The λ_{max} determined from Figure 4 were identical for both TF_{1-218} and TF_LLZ, $\lambda_{max} = 339.2 \pm 0.5$ and 339.3 ± 0.5 nm, respectively. The lack of a change in the λ_{max} indicated a highly similar overall hydrophobic environment for the

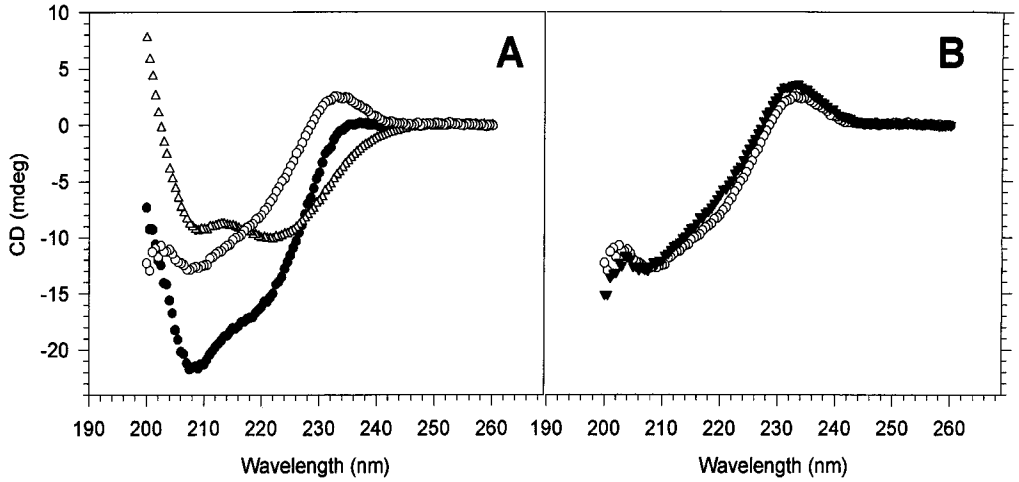

FIGURE 3: Circular dichroism (CD) of TF_LLZ and TF. (A) CD spectra of TF_LLZ (●), TF_{1-218} (○), and LZP (Δ) were recorded in 20 mM potassium phosphate and 10 mM NaCl at pH 7.4 and a concentration of 10 μM. (B) Subtraction of the LZP spectrum from that of TF_LLZ (▼) in comparison to the TF_{1-218} spectrum.

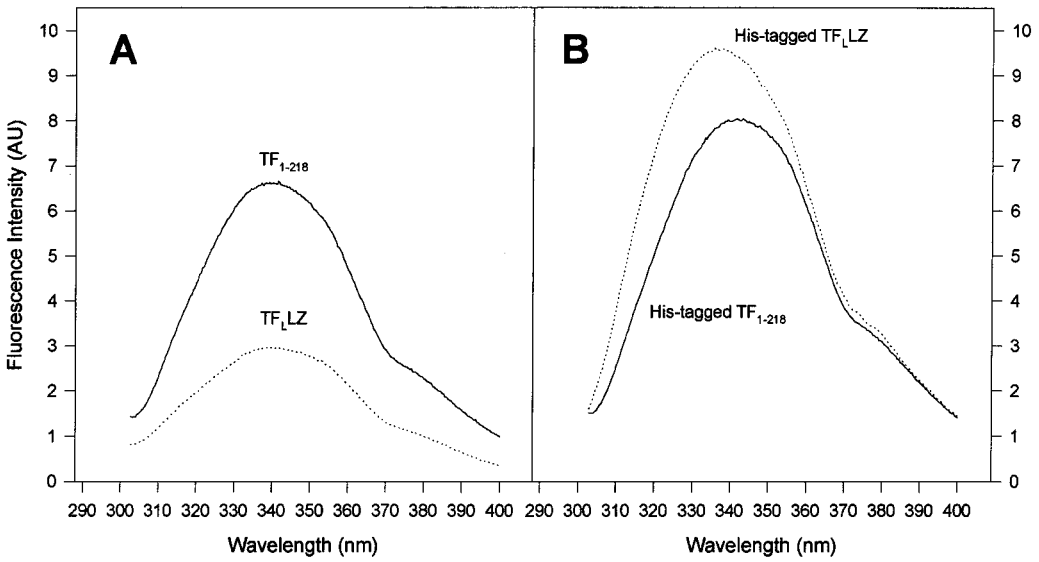

FIGURE 4: Emission fluorescence spectra of TF_LLZ and TF. The proteins were in 10 mM Tris and 150 mM NaCl at pH 7.4 and a concentration of 2 μM. Samples were excited at $\lambda_{ex} = 296$ nm. (A) Spectra of TF_{1-218} and TF_LLZ. (B) Spectra of His-tagged TF_{1-218} and His-tagged TF_LLZ.

tryptophan side chains at positions 14 and 45 in TF_{1-218} and in TF_LLZ. However, the fluorescence emission intensity of TF_LLZ at the λ_{max} was approximately 40% less than that of TF_{1-218}, indicating that one or both of the two fluorescent tryptophans are quenched, by inference from proximity of the TF domain partner in dimeric TF_LLZ. This supports formation of dimeric TF_LLZ in which the TF domains are parallel and in close proximity.

Dimer to Monomer Equilibrium of TF_LLZ. The fluorescence emission spectra of His-tagged TF_{1-218} and His-tagged TF_LLZ were also recorded under identical conditions (Figure 4B). The His tag contains one Trp residue that is located six residues amino proximal to residue 1 of the TF domain or at a maximal distance of 22 Å for an extended polypeptide chain conformation. The λ_{max} of His-tagged TF_{1-218} (341.3 $\pm$ 0.4 nm) (Figure 4B) was red shifted with respect to that of TF_{1-218} (339.2 $\pm$ 0.5 nm), indicating a contribution to the total intrinsic protein fluorescence of the solvent-exposed Trp in the His tag. To the contrary, the spectrum for His-tagged TF_LLZ (Figure 4B) was blue shifted (336.9 $\pm$ 0.2 nm) with respect to TF_LLZ (339.3 $\pm$ 0.5 nm), and the intensity dramatically increased, suggesting a solvent-protected Trp in the His tag as opposed to the solvent-exposed one in monomeric TF. This difference in solvent accessibility of the Trp residue in the His tag between the monomeric and dimeric forms of TF_LLZ was used to determine the dimerization equilibrium. The λ_{max} of the emission spectrum of serial dilutions of His-tagged TF_LLZ was measured and plotted against the protein concentration (Figure 5). The λ_{max} of His-tagged TF_LLZ remained unchanged at high concentrations at which the dimer was predicted to be predominant. As the concentration and therefore the proportion of the TF_LLZ in the dimeric state decreased, the λ_{max} increased, ultimately reaching a value comparable to that of monomeric His-tagged TF_{1-218}. On the other hand, the value of λ_{max} for the monomeric His-tagged TF_{1-218} remained constant for all concentrations analyzed at 340.4 $\pm$ 0.82 nm ($n = 4$). An apparent K_d of 64 nM was calculated from Figure 5, which is within the range of values published for the homodimerization of LZP (*23*)

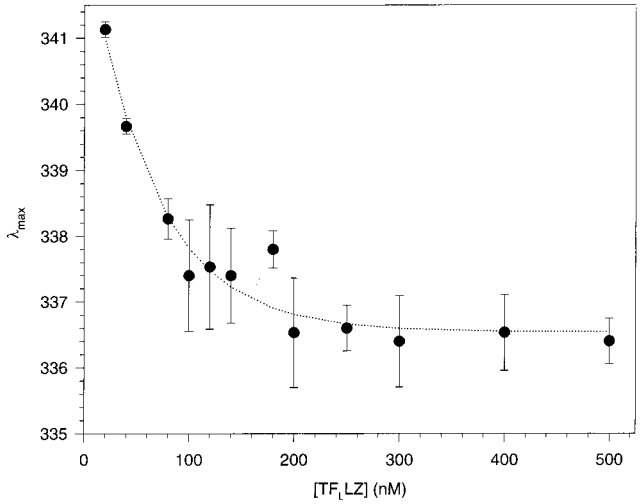

FIGURE 5: Dimer to monomer equilibrium for TF_LLZ. The variation of the λ_{max} of fluorescence emission spectra depending on the concentration of TF_LLZ indicated dimer formation with an apparent K_d of 64 nM.

alone or as a dimerization domain in hybrid proteins (*26*, *27*). As a control, the fluorescence emission spectra of His-tagged TF_{1-218} and TF_LLZ were recorded under identical conditions in the presence and absence of increasing concentrations of LZP. The resulting spectra showed no apparent changes for TF_{1-218}, whereas for TF_LLZ the fluorescence properties reverted to those of TF_{1-218} (data not shown). Thus, these data confirm that the changes in fluorescence observed between His-tagged TF_{1-218} and TF_LLZ originated from dimer formation through the leucine zipper domain of TF_LLZ.

VIIa Stoichiometry with TF in TF_LLZ·VIIa Complexes. The stoichiometry of VIIa binding to the dimer TF_LLZ was analyzed in cross-linking experiments. Figure 6 (top) shows silver-stained SDS−PAGE after BS^3 cross-linking of TF_LLZ incubated with increasing concentrations of VIIa either in the absence (dimeric TF_LLZ, Figure 6A) or in the presence of LZP (monomeric TF_LLZ, Figure 6B). The same samples were also analyzed by Western blotting for the presence of

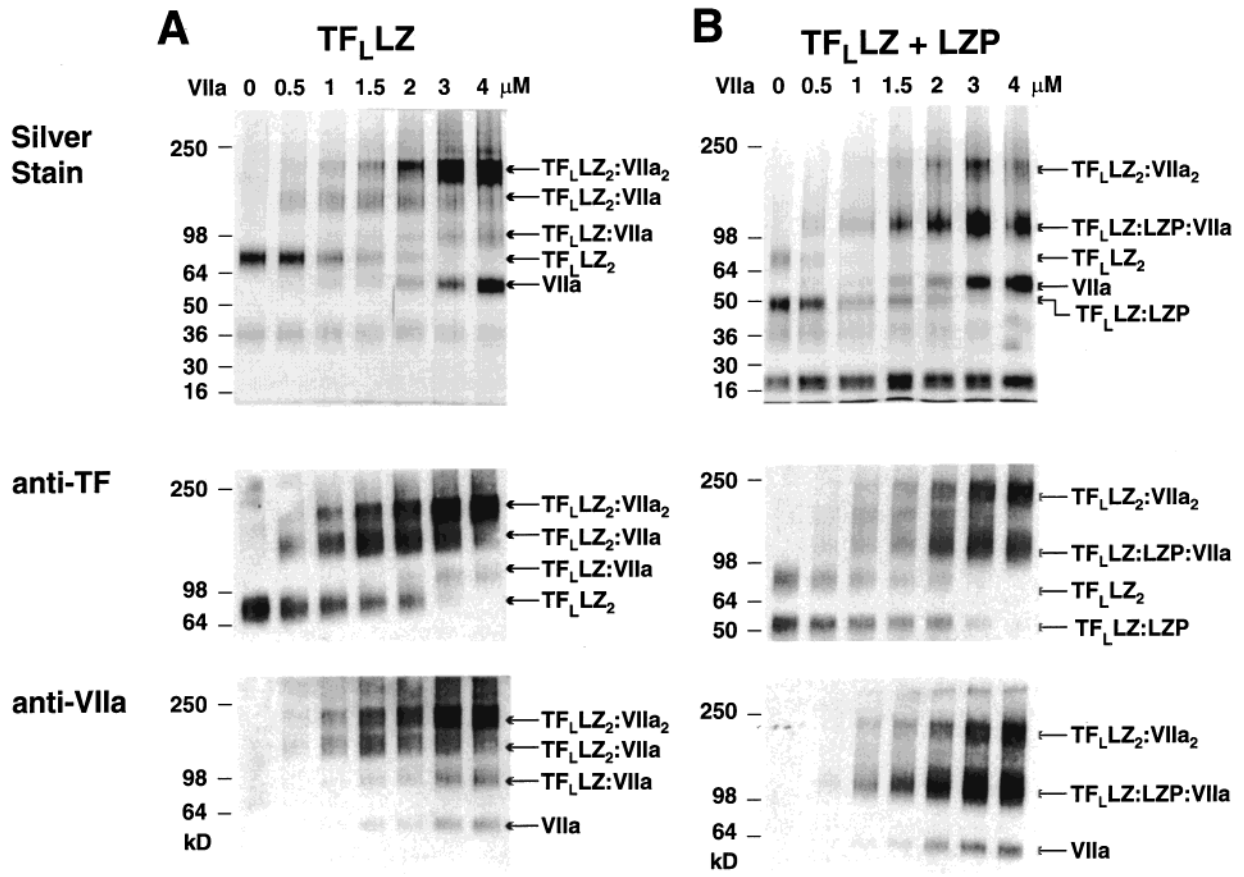

FIGURE 6: Cross-linking of increasing concentrations of VIIa to TF_LLZ. TF_LLZ at 2 μM was incubated with increasing concentrations of VIIa (0−4 μM) in PBS buffer containing 5 mM $CaCl_2$ in the absence (A) or presence (B) of 20 μM of LZP. The samples were cross-linked with BS^3 as described in Figure 2 and separated by 8−16% SDS PAGE. The gels were either silver stained or transferred to a membrane for Western blotting with antibodies against TF (anti-TF) or VIIa (anti-VIIa).

TF (middle) and VIIa (bottom). Dimeric TF_LLZ (TF_LLZ_2) bound two molecules of VIIa, as indicated by the band of ~210 kD (TF_LLZ_2·$VIIa_2$). This band is predominant at high VIIa-to-TF_LLZ ratios (2:1). Two bands of lesser intensity can be identified in Figure 6A as containing TF_LLZ as well as VIIa based on the Western blots. The observed molecular weight (~160 kD) is consistent with a dimeric TF_LLZ with one molecule of VIIa bound (TF_LLZ_2·VIIa). This band is more abundant at substoichiometric concentrations of VIIa with respect to TF_LLZ, and disappears at higher VIIa concentrations. The ~100 kD band is attributed to a TF_LLZ monomer cross-linked to one VIIa molecule (TF_LLZ·VIIa).

In the presence of a 5-fold molar excess of the LZP (Figure 6B), there is a significant decrease in the ~210 kD band (TF_LLZ_2·$VIIa_2$) and the appearance of a new prominent band of ~120 kD, consistent with a trimer TF_LLZ·LZP·VIIa in a 1:1:1 stoichiometry. Quantitative reduction of the tetrameric complex (TF_LLZ_2·$VIIa_2$) upon LZP addition parallels the ratio of monomeric to dimeric TF observed in the absence of VIIa (Figure 2A). Thus, VIIa appears to have no significant effect on the competitive inhibition by LZP of dimer equilibrium of TF_LLZ. This interpretation is further supported by cross-linking experiments that determined the effective concentration of LZP needed to dissociate 50% of the TF_LLZ dimer. The presence of VIIa did not change the concentration dependence for LZP to dissociate the dimer (data not shown). Cross-linking in the presence of macromolecular substrate X at a concentration equimolar to TF also did not change the pattern of cross-linking (data not shown). This infers that X association with the TF domain is not of sufficient duration with the dimeric TF·VIIa complex in solution to permit chemical cross-linking.

Effect of Dimerization on Amidolytic and Proteolytic Activity. Both proteolytic and amidolytic activities of VIIa are greatly enhanced upon association with its cofactor TF (*1*−*3*). Significant changes in the apparent K_d for the TF·VIIa interaction are expected to produce differences in plots of the VIIa amidolytic activity versus the VIIa concentration, measured at a fixed concentration of TF_{1-218} or dimeric TF_L-LZ. In Figure 7A, one observes superimposable curves for the amidolytic activity of TF_{1-218} and of TF_LLZ at a concentration of 300 nM, at which the dimer form is the predominant species. Further, there was no effect of added LZP on the amidolytic activity of VIIa at concentrations of LZP that shifted TF_LLZ from the dimeric to the monomeric state. These results indicate similar affinity of the TF monomer and dimer for VIIa and indicate a comparable cofactor effect on allosteric activation of VIIa's catalytic activity. Because these experiments were carried out at a high TF_LLZ concentration to ensure predominantly dimeric TF_LLZ, more subtle changes in affinity for VIIa could have been masked by these conditions. The inset in Figure 7A indicates that this is unlikely, since the amidolytic activities of TF_LLZ·VIIa at concentrations of TF_LLZ near and below the K_d of dimerization were essentially the same as the activity of TF_{1-218}·VIIa. Under these conditions, addition of LZP was also without influence on the amidolytic activity of VIIa in the presence of TF_LLZ.

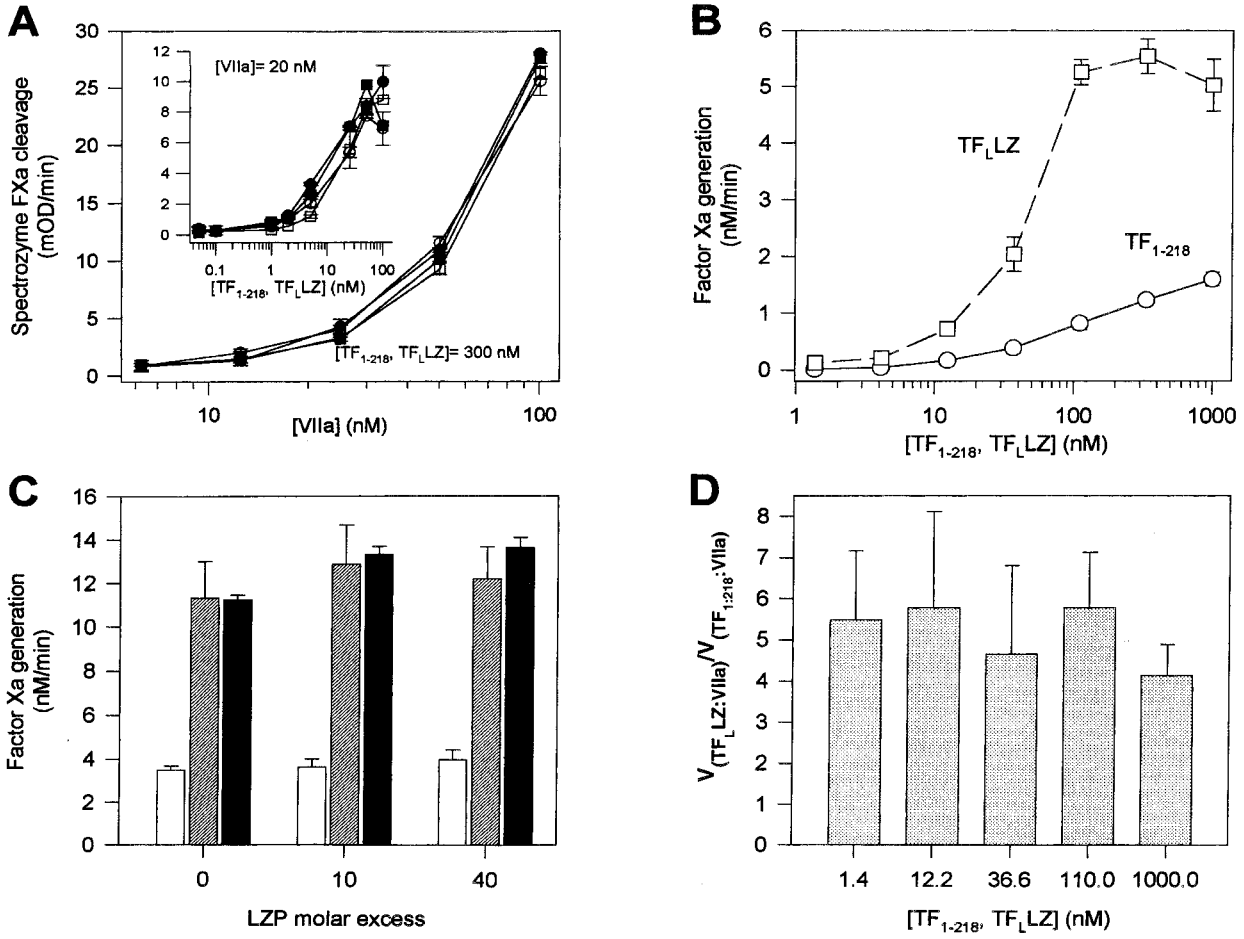

FIGURE 7: Catalytic activity of VIIa in complex with monomeric and dimeric TF. The amidolytic (A) and proteolytic activity (B−D) of the different TF forms complexed to VIIa were measured in a buffer containing TBS, 5 mM $CaCl_2$, and 0.02% BSA. (A) Aliquots (300 nM) of TF_LLZ (□), TF_LLZ + LZP (■), TF_{1-218} (○), and TF_{1-218} + LZP (●) incubated with increasing concentrations of VIIa at 37 °C and followed by determination of the initial rate of hydrolysis of the chromogenic substrate Spectrozyme FXa. The inset shows a similar experiment with a fixed concentration of VIIa (20 nM) and varying TF concentrations. (B) Increasing concentrations of TF_LLZ (□), and TF_{1-218} (○) incubated with 10 nM VIIa at 37 °C. FX was added to a final concentration of 1 μM, and the reaction was quenched by EDTA/TBS buffer for determination of FXa generation by chromogenic assay. (C) Factor X activation by 100 nM of either TF_LLZ (hatched bars), or TF_{1-218} (empty bars), or full-length TF solubilized by Chaps (full bars) with 300 nM VIIa in the presence of the indicated concentrations of LZP was measured at 37 °C. (D) Relative proteolytic activity (V) of TF_LLZ·VIIa versus TF_{1-218}·VIIa dependent on the concentration of TF_LLZ or TF_{1-218}.

The activity of the TF_LLZ·VIIa complex toward its macromolecular substrate factor X is illustrated in Figure 7B−D. In the absence of a phospholipid surface, TF_LLZ was about 5-fold more active as a cofactor for VIIa than TF_{1-218} (Figure 7C). The activity of TF_LLZ is similar to the activity of detergent-solubilized full length TF, which contains transmembrane and cytoplasmic domains (Figure 7C). One possible explanation is an enhancement of proteolytic activity due to dimerization. This effect on the proteolytic activity would equally be achieved by dimerization through the transmembrane domain or the leucine zipper motif. However, when the dimerization equilibrium was altered by addition of LZP (Figure 7C) or dilution (Figure 7D), the activity of TF_LLZ remained approximately 5-fold higher than that of TF_{1-218}. These data indicate that addition of the leucine zipper domain at the C-terminus of the TF extracellular domain increases proteolytic activity of the complex with VIIa by a mechanism that is independent of dimer formation, possibly involving a conformational stabilization of the C-terminus of TF or nonspecific interactions with the Gla domain of substrate X.

It has been proposed that TF dimers on cells have diminished proteolytic activity relative to TF monomers, hypothetically suggested to result from steric hindrance at critical sites for macromolecular substrate docking (*15*). In TF_LLZ, a Gly−Gly−Ala−Ala linker had been introduced between TF residue 220 and the N-terminus of the LZ to provide flexibility and separation between the two domains (Figure 1). This linker might confer TF_LLZ with enough flexibility to avoid the hypothesized inhibitory steric clash. To explore this possibility, a construct lacking the flexible linker was prepared and analyzed. In this construct, TFLZ, residue 219 of TF was directly linked through a single Ala residue to the GCN4 leucine zipper homodimerization domain. This construct should more faithfully mimic the topography of cell surface-expressed TF that is homodimerized through the parallel orientation of its transmembrane regions (*19*). $TFLZ_2$·$VIIa_2$ exhibited an enhancement of amidolytic and proteolytic activity identical to that of TF_L-LZ·VIIa, and the biophysical characteristics in respect to dimer equilibrium also were not influenced by the absence of the linker sequence. TFLZ also reversibly formed dimers

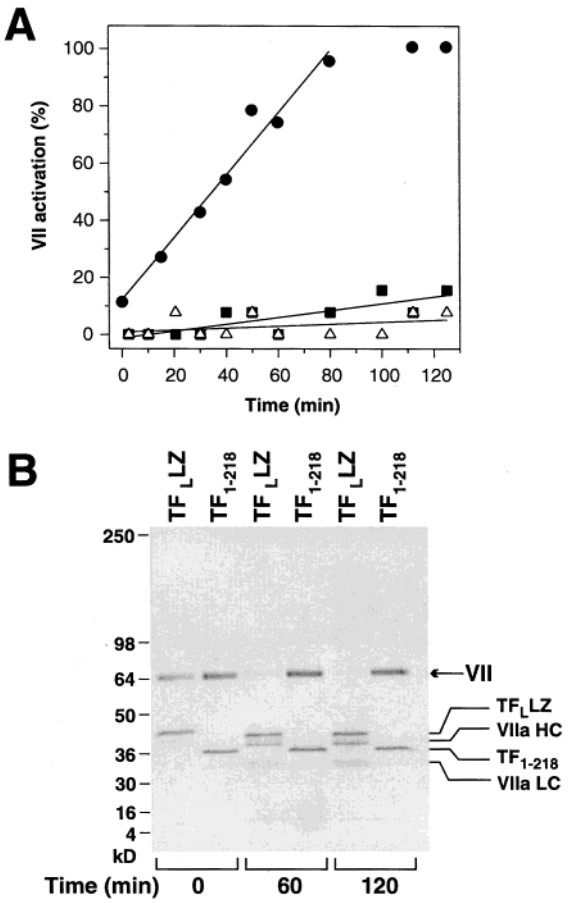

FIGURE 8: Autoactivation of VII by dimeric TF_LLZ. (A) Activation of 300 nM VII measured in the presence of 300 nM of TF_LLZ (●), TF_LLZ with a 50-fold excess of LZP (■), or TF_{1-218} (Δ) in TBS buffer, 5 mM $CaCl_2$, and 0.02% BSA at 37 °C. The activation was quantitated at the indicated times by amidolytic assay. (B) Reduced SDS PAGE analysis of the activation of VII (300 nM) in the presence of 300 nM TF_LLZ or TF_{1-218} in TBS buffer, 5 mM $CaCl_2$, and 0.02% BSA at 37 °C. The positions of zymogen VII, the VIIa heavy (HC) and light chain (LC), TF_LLZ, and TF_{1-218} are indicated in the margin.

as detected by cross-linking and maximally bound two VIIa molecules per dimeric TFLZ (data not shown). Thus, flexibility in the linker between TF and LZ is not masking an inhibitory effect of dimerization on the proteolytic activity of the TF·VIIa complex in solution.

Cofactor Function of TF_LLZ for Activation of VII. The specific proteolytic activation of VII to VIIa by Xa and VIIa is greatly enhanced when bound to TF in a phospholipid membrane (*7*, *28*, *29*). Kinetic studies support the hypothesis that the lateral diffusion of TF·VIIa and TF·VII complexes in the phospholipid bilayer determine the encounter frequency and the activation rate of the cofactor-bound zymogen VII (*7*). Thus, proximity of a TF·VIIa complex to a substrate TF·VII appears to be a major determinant for the efficiency of this form of VII autoactivation. This proximity may be recapitulated by the dimeric TF_LLZ, in solution. We therefore determined whether dimerization of TF is an efficient VII activator in solution. Amidolytic activity was determined as a measure for activation of VII to VIIa. Activation of VII bound to equimolar concentrations of dimeric TF_LLZ (300 nM) occurred in the absence of externally added VIIa (Figure 8A). Since VII preparations have been observed to convert to VIIa in the absence of TF, it is impossible to exclude the presence of trace contaminating VIIa in the VII preparations. Thus, traces of VIIa may have initiated the observed conversion of VII to VIIa. However, VII activation did not take place in the presence of TF_{1-218}, or TF_LLZ in the presence of a 50-fold excess of LZP that dissociates the dimeric TF_LLZ, demonstrating that autoactivation is dependent on dimer formation. VII activation also occurred efficiently in the presence of TFLZ, which lacks the linker insert between the extracellular domain of TF and the leucine zipper (result not shown). The activation of VII was also monitored by SDS−PAGE (Figure 8B) demonstrating that at time zero most VII was intact and that after 120 min all VII is converted to VIIa in the presence of TF_LLZ. In contrast, VII bound to TF_{1-218} remained as single-chain zymogen for the duration of the experiment.

The activation of VII with time was linear (Figure 8A), and the slope did not change significantly when active VIIa at increasing concentrations was added at the beginning of the reaction (data not shown). These data indicate that dissociation events, rather than encounter frequency in solution, are the major determinant of the activation rate. Exchange of VII for VIIa in the tetrameric TF_LLZ_2·$VIIa_2$ complex or dissociation of the leucine zipper could determine the reaction rate. The rate constant for the unfolding of dimeric GCN4 at zero denaturant concentration has been calculated to be 3.3×10^{-3} s^{-1} (*30*), yielding a $t_{1/2}$ of 5 min. A $t_{1/2}$ of 5 min is clearly within the time frame of the measured activation rates of VII. The K_{off} for binding of VIIa to soluble TF is 5.6×10^{-4} s^{-1} (*31*). This $t_{1/2}$ of 30 min is slower but could contribute to some degree within the time frame of the experiments reported here. The dimer dissociation of tetrameric TF_LLZ_2·$VIIa_2$ and TF_LLZ_2·VII_2 complexes and the reassembly into tetrameric TF_LLZ·VII·TF_LLZ·VIIa units thus appears to be the major determinant for the activation rate of VII by TF_LLZ, whereas a minor contribution to the progress of the reaction is expected from exchange of zymogen VII due to dissociation of a molecule of VIIa from the tetrameric TF_LLZ_2·$VIIa_2$ complex.

DISCUSSION

The results presented here support the following conclusions: (i) TF_LLZ forms a reversible dimer with a K_d of approximately 60 nM. The two TF_{1-220} moieties in the TF_LLZ dimer are in a parallel orientation in close proximity, which represents a model for the relative orientation of dimeric TF on a cell surface; (ii) the TF_LLZ dimer can bind two VIIa molecules, and binding of VIIa does not appreciably influence the dimerization equilibrium; (iii) the amidolytic and proteolytic activities of VIIa bound to TF_LLZ are not influenced by dimerization, and consequently, it appears that each TF_LLZ·VIIa unit functions independently in the tetrameric TF_LLZ_2·$VIIa_2$ complex; (iv) dimeric TF_LLZ, unlike monomeric TF_LLZ or soluble TF, efficiently supports autoactivation of VII; (v) flexibility in the linker from TF to the dimerization domain is not required for Xa generation or autoactivation of VII, indicating that the membrane-tethering peptidyl strand of TF (residue 211−219) is of sufficient flexibility to avoid steric clashes.

Fluorescence properties of TF_LLZ demonstrate close proximity of the two TF domains in the TF_LLZ dimer as a result of the parallel orientation that is mediated by the

carboxyl leucine zipper coiled−coil domain (*18*). First, the changes in fluorescence of the Trp present in the His tag at the N-terminus of His-tagged TF_LLZ indicate that the Trp residues from each subunit of the dimeric His-tagged TF_L-LZ are in close proximity. Second, the fluorescence of one or both of the fluorescent tryptophans (Trp 14 and 45) (*25*) in TF_LLZ is quenched by the proximity of the other subunit also suggests that the TF domains are in a parallel orientation and close proximity. Trp 14, which is buried to a large degree, contributes approximately 25% to the total intrinsic protein fluorescence, and Trp 45, which is reasonably exposed, contributes 75% (*25*). The fluorescence of the TF_L-LZ dimer is quenched approximately 40% in comparison to that of TF_{1-218}. Thus, the fluorescence of Trp 14 alone cannot account for the observed degree of quenching. It is more likely that Trp 45 is the candidate fluorophore being quenched in dimeric TF_LLZ. Thus, despite the flexibility provided by the inserted linker and the TF tether region (amino acids: 211−219), the amino terminal extracellular domain modules of two TF molecules must be in close proximity to reduce the solvent accessibility of Trp 45. Since Trp 45 is located within a prominent hydrophobic cluster of residues on the protein surface, one may speculate that a hydrophobic contact is formed between these surface sites of two adjacent TF molecules. However, soluble TF is monomeric, and the proposed hydrophobic interaction thus does not occur in the absence of a carboxyl-terminal dimerization domain that could be naturally provided by the transmembrane domain of TF (*14*). Furthermore, this hydrophobic contact also appears to contribute little binding energy to the dimer formation of TF_LLZ, because the K_d for dimerization (60 nM) is well within the range of established values for leucine zipper domains alone (*23*).

Trp 45 is largely buried in the interface with the VIIa protease domain in the crystal structure of the TF·VIIa complex (*6*). The finding that the stoichiometry of VIIa binding to dimeric TF_LLZ was as expected argues that the hydrophobic patch surrounding Trp 45 does not form a stable interface between two TF molecules sufficient to interfere with VIIa binding and function. This notion is further supported by the finding that the affinity of VIIa for TF_LLZ and soluble TF was similar and that the dimer to monomer transition of the leucine zipper domain in TF_LLZ was not influenced by assembly with VIIa. Nevertheless, Trp 45 is located on the same face of the TF extracellular domain that contributes to association with macromolecular substrates. The access to this more membrane-proximal region, marked by the critical residues Lys 165 and Lys 166, thus might have been restricted in the dimer after binding of VIIa. However, dimerization did not influence the activation of X, demonstrating that dimer formation per se is insufficient to regulate the procoagulant function of TF.

Prior data provided good evidence that the presence of dimeric TF on the cell surface is closely correlated with TF procoagulant activity (*15*). Moreover, Lys residues which are critical for TF procoagulant function are more protected from chemical modifications in cells with higher concentrations of dimeric TF. The finding that dimerization per se is not sufficient to diminish the rate of X activation by the TF·VIIa complex argues that cell surface dimerization of TF does not significantly regulate TF function, but rather reflects a localization of TF in a plasmalemma microenvironment that poorly supports activation of substrate zymogens by the formed TF·VIIa complexes (*13*). A cellular trafficking of TF, together with changes in the membrane phospholipid asymmetry induced by the cell stimulation, may be responsible for the overall enhancement of TF proteolytic function upon agonist stimulation of cells.

Previous studies have clearly established that all TF on the cell membrane can bind VIIa, despite the evidence that only a subpopulation participates in the activation of factor X or IX and thereby initiation of the coagulation cascade (*32*). However, the nonprocoagulant population of cell surface TF does enhance the amidolytic function of the bound VIIa, demonstrating formation of a catalytically active complex with VIIa on these differing plasmalemma microdomains. Considering that nonprocoagulant pools of TF appear to include the dimeric forms, our finding that dimeric TF_LLZ in solution is uniquely potent in promoting autoactivation of VII in solution may suggest biological roles for the sequestered TF in these nonprocoagulant loci on the cell surface membrane. First, the activation of VII to VIIa without concomitant downstream activation of the coagulation pathways may result in a "priming" of the pathway by increasing the concentration of active TF·VIIa complexes that remain on the cell surface awaiting only translocation to a substrate-rich anionic plasmalemma locus. An appropriate stimulus that enhances proteolytic activity may result in a rapid relocation of these complexes to substrate-rich loci with resultant explosive triggering of coagulation as observed in sepsis and other forms of intravascular thrombogenesis. Second, sequestration of TF in a nonprocoagulant environment may serve for nonhemostatic functions. A number of reports have provided evidence that the TF·VIIa complex on cells may activate an as yet unidentified protease activated receptor (PAR) (*33*−*36*). The cellular consequences of TF·VIIa signaling range from MAP kinase activation to Ca^{2+} fluxes and gene induction. Sequestering these processes into a specific microdomain of the cell membrane may be necessary to allow for encounter with the signaling receptors and to separate this pathway from the activation of the procoagulant substrate and the associated feedback inhibition by TF pathway inhibitor (TFPI). Dimeric TF may thus represent the cellular pool of TF that achieves the activation of circulating zymogen VII, as well as elicits direct protease-dependent signaling in cells that express the cognate PAR.

REFERENCES

1. Ruf, W. and Edgington, T. S. (1994) *FASEB J. 8*, 385−390.
2. Edgington, T. S., Dickinson, C. D., and Ruf, W. (1997) *Thromb. Haemost. 78*, 401−405.
3. Ruf, W., and Dickinson, C. D. (1998) *Trends Cardiovasc. Med. 8*, 350−356.
4. Harlos, K., Martin, D. M. A., O'Brien, D. P., Jones, E. Y., Stuart, D. I., Polikarpov, I., Miller, A., Tuddenham, E. G. D., and Boys, C. W. G. (1994) *Nature 370*, 662−666.
5. Muller, Y. A., Ultsch, M. H., Kelley, R. F., and De Vos, A. M. (1994) *Biochemistry 33*, 10864−10870.
6. Banner, D. W., D'Arcy, A., Chene, C., Winkler, F. K., Guha, A., Konigsberg, W. H., Nemerson, Y., and Kirchhofer, D. (1996) *Nature 380*, 41−46.
7. Neuenschwander, P. F., Fiore, M. M., and Morrissey, J. H. (1993) *J. Biol. Chem. 268*, 21489−21492.
8. ten Cate, H., Bauer, K. A., Levi, M., Edgington, T. S., Sublett, R. D., Barzegar, S., Kass, B. L., and Rosenberg, R. D. (1993) *J. Clin. Invest. 92*, 1207−1212.

9. Levi, M., ten Cate, H., Bauer, K. A., van der Poll, T., Edgington, T. S., Büller, H. R., van Deventer, S. J. H., Hack, C. E., ten Cate, J. W., and Rosenberg, R. D. (1994) *J. Clin. Invest. 93*, 114−120.
10. Hamilton, K. K., Hattori, R., Esmon, C. T., and Sims, P. J. (1990) *J. Biol. Chem. 265*, 3809−3814.
11. Bach, R. and Rifkin, D. B. (1990) *Proc. Natl. Acad. Sci. U.S.A. 87*, 6995−6999.
12. Wolberg, A. S., Monroe, D. M., Roberts, H. R., and Hoffman, M. R. (1999) *Blood Coagulation Fibrinolysis 10*, 201−210.
13. Sevinsky, J. R., Rao, L. V. M., and Ruf, W. (1996) *J. Cell. Biol. 133*, 293−304.
14. Roy, S., Paborsky, L. R., and Vehar, G. A. (1991) *J. Biol. Chem. 266*, 4665−4668.
15. Bach, R. R., and Moldow, C. F. (1997) *Blood 89*, 3270−3276.
16. Ruf, W., Miles, D. J., Rehemtulla, A., and Edgington, T. S. (1992) *J. Biol. Chem. 267*, 6375−6381.
17. Roy, S., Hass, P. E., Bourell, J. H., Henzel, W. J., and Vehar, G. A. (1991) *J. Biol. Chem. 266*, 22063−22066.
18. O'Shea, E. K., Klemm, J. D., Kim, P. S., and Alber, T. (1991) *Science 254*, 539−544.
19. Stone, M. J., Ruf, W., Miles, D. J., Edgington, T. S., and Wright, P. E. (1995) *Biochem. J. 310*, 605−614.
20. Dickinson, C.D., Kelly, C.R., Ruf, W. (1996). *Proc. Natl. Acad. Sci. U.S.A. 93*, 14379−14384.
21. Ruf, W. (1994) *Biochemistry 33*, 11631−11636.
22. Waxman, E., Ross, J. B., Laue, T. M., Guha, A., Thiruvikraman, S. V., Lin, T. C., Konigsberg, W. H., and Nemerson, Y. (1992) *Biochemistry 31*, 3998−4003.
23. O'Shea, E. K., Rutkowski, R., and Kim, P. S. (1989) *Science 243*, 538−542.
24. Ruf, W., and Edgington, T. S. (1991) *Proc. Natl. Acad. Sci. U.S.A. 88*, 8430−8434.
25. Hasselbacher, C. A., Rusinova, E., Waxman, E., Rusinova, R., Kohanski, R. A., Lam, W., Guha, A., Du, J., Lin, T. C., Polikarpov, I., Boys, C. W. G., Nemerson, Y., Konigsberg, W. H., and Ross, J. B. A. (1995) *Biophys. J. 69*, 20−29.
26. Blondel, A., and Bedouelle, H. (1991) *Protein Eng. 4*, 457−461.
27. Witte, S., Neumann, F., Krawinkel, U., and Przybylski, M. (1996) *J. Biol. Chem. 271*, 18171−18175.
28. Nakagaki, T., Foster, D. C., Berkner, K. L., and Kisiel, W. (1991) *Biochemistry 30*, 10819−10824.
29. Rao, L. V. M., and Rapaport, S. I. (1988) *Proc. Natl. Acad. Sci. U.S.A. 85*, 6687−6691.
30. Zitzewitz, J. A., Bilsel, O., Luo, J., Jones, B. E., and Matthews, C. R. (1995) *Biochemistry 34*, 12812−12819.
31. Dickinson, C. D., and Ruf, W. (1997) *J. Biol. Chem. 272*, 19875−19879.
32. Le, D. T., Rapaport, S. I., and Rao, L. V. M. (1992) *J. Biol. Chem. 267*, 15447−15454.
33. Camerer, E., Rottingen, J.-A., Iversen, J.-G., and Prydz, H. (1996) *J. Biol. Chem. 271*, 29034−29042.
34. Taniguchi, T., Kakkar, A. K., Tuddenham, E. G. D., Williamson, R. C. N., and Lemoine, N. R. (1998) *Cancer Res. 58*, 4461−4467.
35. Poulsen, L. K., Jacobsen, N., Sorensen, B. B., Bergenhem, N. C. H., Kelly, J. D., Foster, D. C., Thastrup, O., Ezban, M., and Petersen, L. C. (1998) *J. Biol. Chem. 273*, 6228−6232.
36. Sorensen, B. B., Freskgard, P.-O., Nielsen, L. S., Rao, L. V. M., Ezban, M., and Petersen, L. C. (1999) *J. Biol. Chem. 274*, 21349−21354.

BI000986P